Event-Triggered Neuro-Adaptive Cooperative Control for Nonlinear Multi-Agent Systems with Full State Constraints and Prescribed Performance

Meirong Zheng, Jing Hu

College of Information and Intelligent Transportation, Fujian Chuanzheng Communications College, Fuzhou 350002, China

Abstract: This paper proposes an event-triggered adaptive control algorithm, considering the full state constraints and prescribed performance, to address the cooperative tracking problem of a class of non-strict feedback nonlinear multi-agent systems. First, a performance function is designed to allow the tracking error to be converge within a specified range within a preset time. Then, the Barrier Lyapunov function is introduced into the backstepping method, so that all states meet the constraints. This is combined with the dynamic surface technology to solve the "calculation explosion" problem caused by the traditional backstepping method. The radial basis function neural networks are used to deal with the unknown nonlinear function. Finally, based on the Lyapunov stability theory, it is proved that all the signals in the system are semi-globally uniform and ultimately bounded, and the tracking error converges to the bounded neighborhood of zero and satisfies the prescribed performance. At the end, the effectiveness of the proposed control algorithm is verified through simulation results.

Keywords: Multi-Agent Systems, Cooperative Control, Neuro-Adaptive Control, Event-Triggered Control, Prescribed Performance

1. INTRODUCTION

Over the past few decades, the leader-follower problem of nonlinear systems has been an increasingly active research topic because it arises in many applications, such as formations of unmanned aerial vehicles (Wu et al., 2020) and satellite formation flying (Zhou et al., 2013). To improve the leader-following control performance of unknown nonlinear systems, both the preset time control and prescribed performance are necessitated to be considered in the design process.

The leader-follower problem can be regarded as a special type of consensus problem in multi-agent systems (MASs). The leader aims to track the ideal trace, the followers aim to track the leader, and only local information is used to design the controller (Ni and Cheng, 2010; Chen et al., 2020; Zegers et al., 2022). The controllability of a leader-follower network with switching topologies was studied based on switched control system theory. It was demonstrated that the controllability of the whole network does not necessarily rely on that of the network for each specific topology (Liu et al., 2008). The leader-follower problem can be extended to multi-agent formations, and formation can be realized by choosing proper gains and interconnection topologies (Tanner et al., 2004). Most papers dealing with MAS topics focus on linear systems. Admittedly, however, the real-world systems often have nonlinear characteristics to make the algorithms (Isidori, 1985) more practical. A distributed leader-follower algorithm for nonlinear systems with time-varying velocities was designed using observer-based pinning navigation feedback (Yu et al., 2010). The leader-follower formation control problem of underactuated autonomous underwater vehicles, which were considered a special nonlinear system, was studied (Cui et al., 2010). In fact, as stated in (Krstic et al., 1995), most nonlinear systems can be converted into a lower triangular structure (Krstic et al., 1995). In this case, the backstepping method should be an appropriate way to design the controller. The backstepping control method can be used in multi-agent nonlinear systems, such as formation kinematic models (Rego et al., 2016) and nonholonomic mobile robots of a leader-follower scheme (Castro et al., 2009).

To improve the practicability of nonlinear algorithms and the steady-state performance of controlled systems, the state constraints and prescribed performance should be taken as significant factors in designing the controller (Bechlioulis and Rovithakis, 2008, 2014; Song et al., 2017; Zhao et al., 2018). In order to handle the tracking error constraints, the constrained system was transformed into an equivalent unconstrained one through a properly defined output error transformation (Bechlioulis and Rovithakis, 2008). Then, the method for unconstrained systems can be used to solve the stated problem. Bechlioulis *et al.* proposed a state feedback controller for unknown pure feedback systems with capability of prescribed performance (Bechlioulis and Rovithakis, 2014). A barrier Lyapunov function was designed to solve the zero-error tracking problem of a nonlinear system, and the full state constraints were proved to be uniformly prespecified (Zhao et al., 2018). In (Li et al., 2021), adaptive tracking optimal control problem with state constraints is studied and novel barrier optimal performance index functions is proposed to achieve optimal control. Chen *et al.* proposed an adaptive controller for unknown pure-feedback systems with full-state constraints and prescribed performance (Chen and Wang, 2019). Dynamics surface control scheme is developed to remove the problems of "explosion of complexity" (Girosi and Poggio, 1990). Although prescribed performance control has been studied from different perspectives, the problems of state constraint and sparse computation for multi-agent unknown nonlinear systems have not been fully considered.

This paper studies the consensus tracking problem of a class of non-strict feedback MASs with full state constraints, and proposes a neuro-adaptive control algorithm. Our proposed algorithm is superior to existing algorithms in that it fully considers the transformation of the tracking error under the specified performance and can thereby obtain a smaller steady-state error. In addition, the controller design incorporates a fixed threshold event trigger mechanism to produce an adaptive control algorithm based on event trigger. Compared with the case that the controller incorporates a time-varying threshold for event triggering, in contrast, our designed controller used a fixed threshold to trigger the computation of controller. Thus, this design contributes to reduce the communication cost and computational consumption between agents for the triggering threshold. In designing the control algorithm, radial basis function neural networks (RBFNNs) are used to process the unknown nonlinear function in a way that ensures the matching condition is satisfied and the unknown nonlinear function is fitted in the controller design. Further, the dynamics surface technology is introduced to the backstepping technique, to avoid the issue of "calculation explosion" in conventional backstepping methods.

The remainder of this paper is structured as follows. Section 2 presents the preliminaries of this paper and the problem it aims to solve. Section 3 gives details about the proposed neuro-adaptive control algorithm and how a barrier Lyapunov function is used to prove the convergence. In Section 4, the feasibility and effectiveness of the proposed controller structure are verified by numeric simulation. Finally, conclusions are given in Section 5.

2. PRELIMINARIES AND PROBLEM STATEMENT

2.1 Graph Theory

In this paper, we use graph theory to describe the communication topological connections between agents. The directed graph between agents is denoted as $\mathcal{G} = (\mathcal{V}, \mathcal{E}, \mathcal{A})$, where $\mathcal{V} = \{v_1, v_2, \dots, v_N\}$ is the set of N agents, $\mathcal{E} \in \mathcal{V} \times \mathcal{V}$ is the directed edges among agents, and $\boldsymbol{A} = [a_{ij}]^{N\times N}$ is the adjacency matrix. If $(v_j, v_i) \in \mathcal{E}$, then $a_{ij} > 0$, otherwise, $a_{ij} = 0$. The in-degree matrix and the Laplacian matrix of the graph G are defined as $\boldsymbol{D} = \text{diag}\{deg_1, deg_2, \dots, deg_N\}$ and $\boldsymbol{\mathcal{L}} = \boldsymbol{\mathcal{D}} - \boldsymbol{A}$, where $\deg_i = \sum_{j=1}^{N} a_{ij}$ is the in-degree of vertex i. The neighboring node of agent i is defined as $\mathcal{N}_i$.

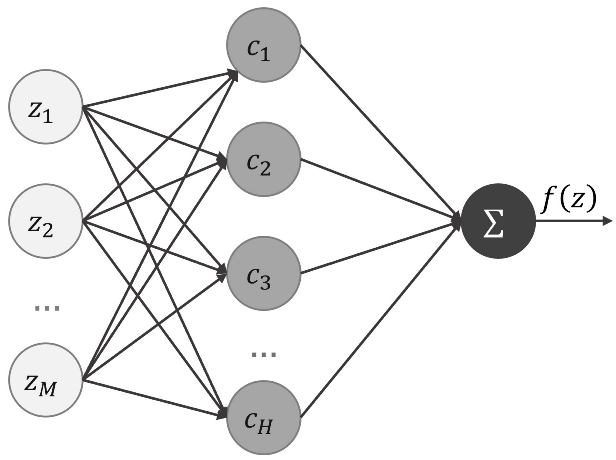

Fig. 1. Structure of radial basis function neural network.

Lemma 1: *If there is a path that can reach all the other nodes from the root node, then the directed graph $\mathcal{G}$ is deemed to have a spanning tree. Let $\mathcal{B} = diag\{a_{1,0}, \cdots, a_{N,0}\}$, where node 0 is the root of the spanning tree, then the matrix $\mathcal{L} + \mathcal{B}$ is non-singular.*

2.2 Notations

This paper uses the following notations:

$\mathbb{R}^n$: n-dimensional vector of real number set.

$\mathbf{1}_n$: n-dimensional column vector with number 1.

$\mathbf{I}_n$: $n \times n$-dimensional identity matrix.

$\text{tr}\{P\}$: The trace of matrix P.

$\{\cdot\}^T$: The transpose of a vector or a matrix.

$\underline{\sigma}(P)$: The smallest singular values of matrix P.

$\bar{\sigma}(P)$: The largest singular values of matrix P.

$\text{diag}\{m_1, m_2, \dots, m_n\}$ is a diagonal matrix with diagonal elements of $m_1, m_2, \dots, m_n$.$\|\cdot\|_1$ is the 1-norm, $\|\cdot\|$ is the Euclidean norm of a vector, and $\|\cdot\|_F$ is the Frobenius norm. Given a matrix $\boldsymbol{A} = [a_{ij}]_{m\times n} \in \mathbb{R}^{m\times n}$, the 1-norm is

$$\|\boldsymbol{A}\|_1 = \max_{1\le j\le n} \sum_{i=1}^{m} |a_{ij}|,$$

and the Frobenius norm is defined as the sum of the squares of the absolute values of the elements of a matrix, i.e.,

$$\|\boldsymbol{A}\|_F = \sqrt{\text{tr}\big(\boldsymbol{A}^T\boldsymbol{A}\big)} = \sqrt{\sum_{i=1}^{m}\sum_{j=1}^{n} |a_{ij}|^2}$$

2.3 Radial Basis Function Neural Networks

As shown in Fig. 1, radial basis function neural networks (RBFNNs) are used to approximate the continuous nonlinear term based on the universal approximation theorem (Girosi and Poggio, 1990)

$$f(\mathcal{Z}) = \mathbf{W}^T\phi(\mathcal{Z}) \tag{1}$$

where $\phi(\mathcal{Z}) = \big[\phi_1(\mathcal{Z}), \phi_2(\mathcal{Z}), \cdots, \phi_H(\mathcal{Z})\big]^T$ is the radial basis vector with H being the number of hidden neurons.

$$\phi_i(\mathcal{Z}) = \exp\left(-\frac{(\mathcal{Z}-c_i)^T(\mathcal{Z}-c_i)}{\omega_i^2}\right) \tag{2}$$

where c_i and ω_i are the center and width of Gaussian function, respectively, and $\mathbf{W} \in \mathbb{R}^H$ denotes the weights of the RBFNNs. According to the universal approximation theorem, there exists an ideal weight vector $\tilde{\mathbf{W}}$ and any sufficiently small constant δ which make the following equation hold:

$$f(\mathcal{Z}) = \tilde{\mathbf{W}}^T\phi(\mathcal{Z}) + \delta(\mathcal{Z}) \tag{3}$$

The optimal weight value of the RBFNN can be defined as

$$\mathbf{W} = \arg\min_{W\in R^n}[\sup\|W^T\Phi - f(\mathcal{Z})\|] \tag{4}$$

To realize this approximation, an adaptive neural network is designed in this paper, and the neural weights will be updated through an adaptive law proposed later in this paper.

2.4 Problem Statement

For a class of MASs with N homogeneous agents, the i-th agent can be described by the following M-th order non-strict feedback nonlinear system:

$$\begin{aligned}\dot{x}_{i,m} &= x_{i,m+1} + f_{i,m}(x_i), m = 1,2,\cdots,M-1\\ \dot{x}_{i,M} &= u_i + f_{i,M}(x_i)\\ y_i &= x_{i,1}\end{aligned} \tag{5}$$

where $x_i = [x_{i,1}, x_{i,2}, \ldots, x_{i,M}]^{\mathrm{T}} \in \mathbb{R}^M$ denotes the state vector of the i-th agent; $y_i \in \mathbb{R}$ and $u_i \in \mathbb{R}$ represent the agent output and control input variables to the i-th agent, respectively; $f_{i,m}(x_i), i = 1,2,\cdots,N; m = 1,2,\cdots,M$ are unknown smooth nonlinear functions.

Assumption 1: The directed graph $\mathcal{G}$ has a spanning tree. The desired trajectory y_0 of the leader agent (labeled as node 0) can only be directly obtained by some follower agents. y_0 is known, and its M-order derivatives are all continuous and bounded.

Definition 1: If for any prior compact set $\Omega \in \mathbb{R}^M, x(0) \in \Omega$, there is a bounded $\varepsilon > 0$ and a constant $C(\varepsilon, x(0))$ such that

$$\| x(t) \| < \varepsilon, \forall t \geq t_0 + C$$

then the solution of the system (5) is semi-globally uniform and ultimately bounded.

3. EVENT-TRIGGERED CONTROL ALGORITHM DESIGN

Using the backstepping method and dynamic surface technology, this paper designs an event-triggered adaptive control algorithm to enable MASs to realize the following control goals: 1) The output of all agents can track the desired trajectory and meet the prescribed performance; 2) All signals in the system are semi-globally uniform and ultimately bounded.

Define

$$\begin{aligned}e_{i,1} &= \sum_{j\in\mathcal{N}_i} a_{i,j}(y_i - y_j) + a_{i,0}(y_i - y_0)\\ \vartheta_{i,m} &= x_{i,m} - z_{i,m}\\ \lambda_{i,m} &= z_{i,m} - \alpha_{i,m-1}, m = 2,3,\cdots,M.\end{aligned} \tag{6}$$

where $e_{i,1}$ is the tracking error, $\vartheta_{i,m}$ is the virtual error surface, $z_{i,m}$ denotes the output signal of first-order filter, and $\lambda_{i,m}$ and $\alpha_{i,m-1}$ are the filter error and virtual control signal, respectively.

We use the following inequality to define the prescribed performance:

$$-\delta_{\min}\mu(t) < e_{i,1}(t) < \delta_{\max}\mu(t), \forall t > 0 \tag{7}$$

where both $\delta_{\min}$ and $\delta_{\max}$ are adjustable parameters, and

$$\mu(t) = (\mu_0 - \mu_\infty)\exp(-vt) + \mu_\infty \tag{8}$$

is a bounded and strictly monotonically decreasing function. $v, \mu_0 = \mu(0), \mu_\infty$ are positive real numbers. Select the appropriate μ_0, such that $\mu_0 > \mu_\infty$ and $-\delta_{\min}\mu(0) < e_{i,1}(0) < \delta_{\max}\mu(0)$.

To meet the prescribed performance, the following equivalent transformation is carried out:

$$e_{i,1}(t) = \mu(t)\Phi_i(\zeta_i(t)), \forall t \leq 0 \tag{9}$$

where $\zeta_i(t)$ is the transformation error, and $\Phi_i(\zeta_i(t)) = \frac{\delta_{\max}\exp(\zeta_i(t)) - \delta_{\min}\exp(\zeta_i(t))}{\exp(\zeta_i(t)) + \exp(-\omega_i(t))}$. The function $\Phi_i(\zeta_i(t))$ is strictly monotonically increasing, and $\frac{\partial\Phi_i}{\partial\zeta_i} = \frac{2(\delta_{\max}+\delta_{\min})}{\left(\exp(\zeta_i(t))+\exp(-\omega_i(t))\right)^2} > 0$. Thus

$$\zeta_i(t) = \Phi_i^{-1}\left(\frac{e_{i,1}(t)}{\mu_i(t)}\right) = \frac{1}{2}\ln\frac{\phi_i + \delta_{\min}}{\delta_{\max} - \Phi_i} \tag{10}$$

and its derivative is

$$\dot{\zeta}_i(t) = r_i\left(\dot{e}_{i,1} - \frac{\dot{\mu}e_{i,1}}{\mu}\right) \tag{11}$$

where $r_i = \frac{1}{2\mu}\left[\frac{1}{\Phi_i+\delta_{\min} - \frac{1}{\Phi_i - \delta_{\max}}}\right]$.

Define

$$\vartheta_{i,1}(t) = \zeta_i(t) - \frac{1}{2}\ln\frac{\delta_{\min}}{\delta_{\max}} \tag{12}$$

Thus, its derivative is

$$\dot{\vartheta}_{i,1}(t) = r_i\left(\dot{e}_{i,1} - \frac{\dot{\mu}e_{i,1}}{\mu}\right) \tag{13}$$

Define adaptive parameter

$$\theta^*_{i,m} = \| W^*_{i,m} \|^2, m = 1,2,\ldots,M \tag{14}$$

where $W^*_{i,m}$ is the ideal weight of RBFNNs, $\hat{\theta}_{i,m}$ is the estimation of $\theta^*_{i,m}$, and $\tilde{\theta}_{i,m} = \theta^*_{i,m} - \hat{\theta}_{i,m}$.

Lemma 2: *For any positive constant k_{bl}, if it satisfies $|\vartheta_{i,l}| < k_{bl}, \vartheta_{i,l} \in \mathbb{R}$, then the following inequality holds:*

$$\log\frac{k_{bl}^2}{k_{bl}^2 - \vartheta_{i,l}^2} < \frac{\vartheta_{i,l}^2}{k_{bl}^2 - \vartheta_{i,l}^2} \tag{15}$$

Lemma 3: *Let $\vartheta_1 = [\vartheta_{1,1}, \vartheta_{2,1}, \ldots, \vartheta_{N,1}]^T$, $y = [y_1, y_2, \ldots, y_N]^T$, $\bar{y}_0 = [y_0, y_0, \ldots, y_0]^T \in \mathbb{R}^N$, then*

$$\| y - \bar{y}_0 \| \leq \frac{\| s_1 \|}{\underline{\sigma}(\mathcal{L}+\mathcal{B})} \tag{16}$$

where $\underline{\sigma}(\mathcal{L}+\mathcal{B})$ is the minimal singular value of matrix $\mathcal{L}+\mathcal{B}$.

Lemma 4: *(Young's Inequality). With $\forall(x,y) \in \mathbb{R}^n$, the following inequality holds:*

$$xy \leq \frac{p^a}{a}|x|^a + \frac{1}{bp^b}|y|^b \tag{17}$$

where $p > 0, a > 1, b > 1, (a-1)(b-1) = 1$.

The event-triggered adaptive control algorithm is designed with the following steps:

Step 1: Choose a barrier Lyapunov function as

$$V_{i,1} = \frac{1}{2}\log\frac{k_{bl}^2}{k_{bl}^2 - \vartheta_{i,1}^2} + \frac{1}{2}\tilde{\theta}_{i,1}^2 \tag{18}$$

Thus,

$$\dot{V}_{i,1} = \frac{\vartheta_{i,1} r_i}{k_{bl}^2 - \vartheta_{i,1}^2}\Bigg[(d_i + a_{i,0})(\vartheta_{i,2} + \lambda_{i,2} + \alpha_{i,1}) + \bar{f}_{i,1} - \sum_{j\in\mathcal{N}_i} a_{i,j}x_{j,2} - a_{i,0}\dot{y}_0 - \frac{\dot{\mu}e_{i,1}}{\mu}\Bigg] - \tilde{\theta}_{i,1}\dot{\hat{\theta}}_{i,1} \tag{19}$$

where $\bar{f}_{i,1} = (d_i + a_{i,0})f_{i,1}(x_i) - \sum_{j\in\mathcal{N}_\rangle} a_{i,j}f_{j,1}(x_j)$.

We use RBFNNs to approximate the term $\bar{f}_{i,1}$,

$$\bar{f}_{i,1} = \mathbb{W}_{i,1}^T\phi_{i,1}(\mathcal{Z}_{i,1}) + \delta(\mathcal{Z}_{i,1}) \tag{20}$$

According to Lemmas 2 and 4, we have

$$\begin{aligned}\bar{f}_{i,1}\frac{\vartheta_{i,1}r_i}{k_{bl}^2 - \vartheta_{i,1}^2} \leq& \frac{r_i^2 s_{i,1}^2 \parallel \tilde{\mathbf{W}}_{i,1}\parallel^2 \phi_{i,1}^T(\mathcal{Z}_{\rangle,\infty})\phi_{i,1}(\mathcal{Z}_{i,1})}{2p_{i,1}^2(k_{bl}^2 - \vartheta_{i,1}^2)^2} \\ &+ \frac{1}{2}p_{i,1}^2 + \frac{r_i^2 s_{i,1}^2}{2(k_{bl}^2 - \vartheta_{i,1}^2)^2} + \frac{1}{2}\bar{\varepsilon}_{i,1}^2 \\ \leq& \frac{r_i^2 s_{i,1}^2\theta_{i,1}^*\phi_{i,1}^T(X_{i,1})\phi_{i,1}(X_{i,1})}{2p_{i,1}^2(k_{bl}^2 - \vartheta_{i,1}^2)^2} \\ &+ \frac{r_i^2 s_{i,1}^2}{2(k_{bl}^2 - \vartheta_{i,1}^2)^2} + \frac{p_{i,1}^2 + \bar{\varepsilon}_{i,1}^2}{2}\end{aligned} \tag{21}$$

where $X_{i,1} = [x_{i,1}, x_{j,1}]^T$.

$$\begin{aligned}\frac{(d_i + a_{i,0})r_i s_{i,1}}{k_{bl}^2 - \vartheta_{i,1}^2}\big(\vartheta_{i,2} + \lambda_{i,2}\big) \leq& \frac{(d_i + a_{i,0})^2 r_i^2 s_{i,1}^2}{2(k_{bl}^2 - \vartheta_{i,1}^2)^2} \\ &+ \frac{\vartheta_{i,2}^2 + \lambda_{i,2}^2}{2}\end{aligned} \tag{22}$$

The virtual control signal $\alpha_{i,1}$ and adaptive control protocol $\dot{\hat{\theta}}_{i,1}$ for the first step of the backstepping method design are

$$\begin{aligned}\alpha_{i,1} =& \frac{1}{d_i + a_{i,0}}\Bigg[-\frac{c_{i,1}\vartheta_{i,1}}{r_i} - \frac{r_i s_{i,1}}{2(k_{bl}^2 - \vartheta_{i,1}^2)} \\ &- \frac{r_i s_{i,1}}{2p_{i,1}^2(k_{bl}^2 - \vartheta_{i,1}^2)}\hat{\theta}_{i,1}\phi_{i,1}^T(X_{i,1})\phi_{i,1}(X_{i,1}) \\ &- \frac{(d_i + a_{i,0})^2 r_i s_{i,1}}{k_{bl}^2 - \vartheta_{i,1}^2} + a_{i,0}\dot{y}_0 \\ &+ \sum_{j\in\mathcal{N}_i} a_{i,j}x_{j,2} + \frac{\dot{\mu}e_{i,1}}{\mu}\Bigg]\end{aligned} \tag{23}$$

$$\dot{\hat{\theta}}_{i,1} = \frac{r_i^2 s_{i,1}^2}{2p_{i,1}^2(k_{bl}^2 - \vartheta_{i,1}^2)^2}\phi_{i,1}^T(X_{i,1})\phi_{i,1}(X_{i,1}) - \sigma_{i,1}\hat{\theta}_{i,1} \tag{24}$$

where $p_{i,1}, c_{i,1}$ and $\sigma_{i,1}$ are all the positive designed parameters.

Substituting (21)∼(24) to (19), we have

$$\dot{V}_{i,1} \leq \frac{c_{i,1}\vartheta_{i,1}^2}{k_{bl}^2 - \vartheta_{i,1}^2} + \frac{1}{2}\vartheta_{i,2}^2 + \frac{1}{2}\lambda_{i,2}^2 + \frac{1}{2}p_{i,1}^2\frac{1}{2}\bar{\varepsilon}_{i,1}^2 + \sigma_{i,1}\tilde{\theta}_{i,1}\hat{\theta}_{i,1} \tag{25}$$

Step 2: Based on the dynamic surface technology, the following first-order filter is defined to solve the "computational explosion" problem in the backstepping method:

$$\begin{aligned}\tau_{i,2}\dot{z}_{i,2} + z_{i,2} &= \alpha_{i,1}, \\ z_{i,2}(0) &= \alpha_{i,1}(0)\end{aligned} \tag{26}$$

where $\tau_{i,2}$ is a positive designed parameter. Since $\lambda_{i,2} = z_{i,2} - \alpha_{i,1}$, we have $\dot{z} + i, 2 = \frac{\lambda_{i,2}}{\tau_{i,2}}$, and

$$\dot{\varepsilon}_{i,2} = -\frac{\lambda_{i,2}}{\tau_{i,2}} + \gamma_{i,2}(\cdot) \tag{27}$$

where $\gamma_{i,2}(\cdot) = -\dot{s}_{i,1}$ is a continuous function.

Remark 1. After $\alpha_{i,1}$ is derived from step 1, the derivative must be calculated in the next virtual control signal design process, and the virtual control signal must be repeatedly derived in each subsequent step. This results in a "calculation explosion" problem. The dynamic surface technology is introduced to pass the virtual control signal through a first-order low-pass filter to obtain its estimated value $z_{i,2}$. In the subsequent design process, the estimated value can be used to replace the virtual control signal to avoid derivation, thereby simplifying the controller structure.

Choose a Barrier Lyapunov function for the m-th ($m = 2, 3, \cdots, M-1$) step,

$$V_{i,m} = V_{i,m-1} + \frac{1}{2}\log\frac{k_{bm}^2}{k_{bm}^2 - \vartheta_{i,m}^2} + \frac{1}{2}\tilde{\theta}_{i,m}^2 + \frac{1}{2}\lambda_{i,m}^2 \tag{28}$$

According to (5), (6) and (28), we have

$$\begin{aligned}\dot{V}_{i,m} =& \dot{V}_{i,m-1} + \frac{\vartheta_{i,m}}{k_{bm}^2 - \vartheta_{i,m}^2}\big[\vartheta_{i,m+1} + \lambda_{i,m+1} + \alpha_{i,m} \\ &+ f_{i,m}(x_i) - \dot{z}_{i,m}\big] - \tilde{\theta}_{i,m}\dot{\hat{\theta}}_{i,m} \\ &+ \lambda_{i,m}\Bigg[-\frac{\lambda_{i,m}}{\tau_{i,m}} + \gamma_{i,m}(\cdot)\Bigg]\end{aligned} \tag{29}$$

From Lemmas 2 and 4, we can get

$$\begin{aligned}\frac{\vartheta_{i,m}f_{i,m}(x_i)}{k_{bm}^2 - \vartheta_{i,m}^2} \leq& \frac{\vartheta_{i,m}^2\theta_{i,m}^*\phi_{i,m}^T(\bar{x}_{i,m})\phi_{i,m}(\bar{x}_{i,m})}{2p_{i,m}^2(k_{bm}^2 - \vartheta_{i,m}^2)^2} \\ &+ \frac{\vartheta_{i,m}^2}{2(k_{bm}^2 - \vartheta_{i,m}^2)^2} + \frac{1}{2}p_{i,m}^2 + \frac{1}{2}\bar{\varepsilon}_{i,m}^2\end{aligned} \tag{30}$$

$$\frac{\vartheta_{i,m}(\vartheta_{i,m+1} + \lambda_{i,m+1})}{k_{bm}^2 - \vartheta_{i,m}^2} \leq \frac{1}{2}\vartheta_{i,m+1}^2 + \frac{1}{2}\lambda_{i,m+1}^2 + \frac{\vartheta_{i,m}^2}{(k_{bm}^2 - \vartheta_{i,m}^2)^2} \tag{31}$$

The virtual control signal $\alpha_{i,m}$ and adaptive control protocol $\dot{\hat{\theta}}_{i,m}$ of the m-th step are designed as

$$\begin{aligned}\alpha_{i,m} =& - c_{i,m}\vartheta_{i,m} - \frac{3s_{i,m}}{2(k_{bm}^2 - \vartheta_{i,m}^2)} \\ & - \frac{\vartheta_{i,m}\hat{\theta}_{i,m}\phi_{i,m}^T(\bar{x}_{i,m})\phi_{i,m}(\bar{x}_{i,m})}{2p_{i,m}^2(k_{bm}^2 - \vartheta_{i,m}^2)} \\ & - \frac{k_{bm}^2 - \vartheta_{i,m}^2}{2}\vartheta_{i,m} + \dot{z}_{i,m} \end{aligned} \tag{32}$$

$$\dot{\hat{\theta}}_{i,m} = \frac{\vartheta_{i,m}^2}{2p_{i,m}^2(k_{bm}^2 - \vartheta_{i,m}^2)^2}\phi_{i,m}^T(\bar{x}_{i,m})\phi_{i,m}(\bar{x}_{i,m}) - \sigma_{i,m}\hat{\theta}_{i,m} \tag{33}$$

where $p_{i,m}, c_{i,m}$ and $\sigma_{i,m}$ are positive designed parameters. Based on the idea of recursion, we can substitute (25),(30)-(33) into (29) to get

$$\begin{aligned}\dot{V}_{i,m} \leq & - \sum_{l=1}^{m}\frac{c_{i,l}\vartheta_{i,l}^2}{k_{bl}^2 - \vartheta_{i,l}^2} + \sum_{l=1}^{m}\sigma_{i,l}\tilde{\theta}_{i,l}\hat{\theta}_{i,l} \\ & + \sum_{l=2}^{m}\left[- \frac{\lambda_{i,l}^2}{\tau_{i,l}} + \lambda_{i,l}\gamma_{i,l}(\cdot)\right] \\ & + \frac{1}{2}\sum_{l=2}^{m+1}\lambda_{i,l}^2 + \frac{1}{2}\sum_{l=1}^{m}(p_{i,l}^2 + \bar{\varepsilon}_{i,l}^2) + \frac{1}{2}\vartheta_{i,m+1}^2 \end{aligned} \tag{34}$$

Step 3: Similar to step 2, define the filter as

$$\tau_{i,m+1}\dot{z}_{i,m+1} + z_{i,m+1} = \alpha_{i,m}, \quad z_{i,m+1}(0) = \alpha_{i,m}(0)$$

where $\tau_{i,m+1}$ is a positive designed parameter. With $\lambda_{i,m+1} = z_{i,m+1} - \alpha_{i,m}$, we have $\dot{z}_{i,m+1} = \frac{\lambda_{i,m+1}}{\tau_{i,m+1}}$, and thus

$$\dot{\lambda}_{i,m+1} = -\frac{\lambda_{i,m+1}}{\tau_{i,m+1}} + \gamma_{i,m+1}(\cdot) \tag{35}$$

where $\gamma_{i,m+1}(\cdot) = -\dot{s}_{i,m}$ is a continuous function.

Choose the barrier Lyapunov function for the M-th step as

$$V_{i,M} = V_{i,M-1} + \frac{1}{2}\log\frac{k_{bM}^2}{k_{bM}^2 - \vartheta_{i,M}^2} + \frac{1}{2}\tilde{\theta}_{i,M}^2 + \frac{1}{2}\lambda_{i,M}^2 \tag{36}$$

so the derivative of $V_{i,M}$ is

$$\begin{aligned}\dot{V}_{i,M} =& \dot{V}_{i,M-1} + \frac{\vartheta_{i,M}}{k_{bM}^2 - \vartheta_{i,M}^2}\left(u_i + f_{i,M}(x_i) - \dot{z}_{i,M}\right) \\ & + \left[- \frac{\lambda_{i,M}^2}{\tau_{i,M}} + \lambda_{i,M}\gamma_{i,M}(\cdot)\right] - \tilde{\theta}_{i,M}\dot{\hat{\theta}}_{i,M} \end{aligned} \tag{37}$$

According to Lemma 4, we have

$$\begin{aligned}\frac{\vartheta_{i,M}f_{i,M}(x_i)}{k_{bM}^2 - \vartheta_{i,M}^2} \leq & \frac{\vartheta_{i,M}^2\theta_{i,M}^*\phi_{i,M}^T(x_i)\phi_{i,M}(x_i)}{2p_{i,M}(k_{bM}^2 - \vartheta_{i,M}^2)^2} \\ & + \frac{\vartheta_{i,M}^2}{2(k_{bM}^2 - \vartheta_{i,M}^2)^2} + \frac{1}{2}p_{i,M}^2 + \frac{1}{2}\bar{\varepsilon}_{i,M}^2 \end{aligned} \tag{38}$$

Design the adaptive control protocol as

$$\omega_i(t) = \alpha_{i,M} - \bar{m}_i\tanh\left[\frac{\vartheta_{i,M}\bar{m}_i}{\epsilon_i(k_{bM}^2 - \vartheta_{i,M}^2)}\right] \tag{39}$$

$$\begin{aligned}\alpha_{i,M} =& - c_{i,M}\vartheta_{i,M} - \frac{\vartheta_{i,M}}{2(k_{bM}^2 - \vartheta_{i,M}^2)} \\ & - \frac{\vartheta_{i,M}\hat{\theta}_{i,M}\phi_{i,M}^T(x_i)\phi_{i,M}(x_i)}{2p_{i,M}^2(k_{bM}^2 - \vartheta_{i,M}^2)} \\ & - \frac{k_{bM}^2 - \vartheta_{i,M}^2}{2}\vartheta_{i,M} + \dot{z}_{i,M} \end{aligned} \tag{40}$$

$$\begin{aligned}\dot{\hat{\theta}}_{i,M} =& \frac{\vartheta_{i,M}^2}{2p_{i,M}^2(k_{bM}^2 - \vartheta_{i,M}^2)}\phi_{i,M}^T(x_i)\phi_{i,M}(x_i) \\ & - \sigma_{i,M}\hat{\theta}_{i,M} \end{aligned} \tag{41}$$

Define the event trigger mechanism as

$$u_i(t) = \omega_i(t_k), \forall t \in [t_k, t_{k+1} \tag{42}$$

$$t_{k+1} = \inf\{t \in \mathbb{R} | \quad |\varrho(t)| \geq m_i\}, t_1 = 0. \tag{43}$$

where $e_i(t) = \omega_i(t) - u_i(t)$ denotes the measurement error, and $p_{i,M}, c_{i,M}, \sigma_{i,M}, \epsilon_i$ and $\bar{m}_i$ are all the positive designed parameters which make the inequality $m_i < \bar{m}_i$ hold. The event-triggered time is defined as $t_k, k \in \mathbb{Z}^+$. That is, when the condition of (43) is triggered, the control signal is updated to $u_i(t_{k+1})$, and when $t \in [t_k, t_{k+1})$, the control signal remains unchanged as $\omega_i(t_k)$. Therefore, there is a continuous time-varying constant $\tau(t_k)$ that satisfies $\tau(t_k) = 0, \tau(t_{k+1}) = \pm, |\tau(t)| \leq 1, \forall t \in [t_k, t_{k+1})$ and makes the equation $\omega_i(t) = u_i(t) + \tau(t)m_i$ hold. We get

$$\begin{aligned}\dot{V}_{i,M} =& \dot{V}_{i,M} - \frac{c_{i,M}\vartheta_{i,M}^2}{k_{bM}^2 - \vartheta_{i,M}^2} - \frac{\vartheta_{i,M}^2}{2} + \sigma_{i,M}\tilde{\theta}_{i,M}\hat{\theta}_{i,M} \\ & + 0.2785\epsilon_i + \left[- \frac{\lambda_{i,M}^2}{\tau_{i,M}} + \lambda_{i,M}\gamma_{i,M}(\cdot)\right] \\ & + \frac{1}{2}p_{i,M}^2 + \frac{1}{2}\bar{\varepsilon}_{i,M}^2 \\ \leq & \sum_{l=1}^{M}\frac{-c_{i,l}\vartheta_{i,l}^2}{k_{bM}^2 - \vartheta_{i,M}^2} + \sum_{l=2}^{M}\left[- \frac{\lambda_{i,l}^2}{\tau_{i,l}} + \lambda_{i,l}\gamma_{i,l}(\cdot)\right] \\ & + \sum_{l=1}^{M}\sigma_{i,l}^M\sigma_{i,l}\tilde{\theta}_{i,l}\hat{\theta}_{i,l} + \frac{1}{2}\sum_{l=2}^{2}\lambda_{i,l}^2 + \frac{1}{2}\sum_{l=1}^{M}\left(p_{i,l}^2 + \bar{\varepsilon}_{i,l}^2\right) \\ & + 0.2785\epsilon_i \end{aligned} \tag{44}$$

According to Lemma 4, the following inequalities hold:

$$\sigma_{i,l}\tilde{\theta}_{i,l}\hat{\theta}_{i,l} \leq -\frac{\sigma_{i,l}\tilde{\theta}_{i,l}^2}{2} + \frac{\sigma_{i,l}\theta_{i,l}^{*2}}{2} \tag{45}$$

$$\lambda_{i,l}\gamma_{i,l}(\cdot) \leq \frac{\lambda_{i,l}^2\gamma_{i,l}^2(\cdot)}{2} + \frac{1}{2} \tag{46}$$

and according to Lemma 2, the following inequality holds:

$$-\frac{c_{i,l}\vartheta_{i,l}^2}{k_{bM}^2 - \vartheta_{i,M}^2} \leq -c_{i,l}\log\frac{k_{bl}^2}{k_{bM}^2 - \vartheta_{i,M}^2} \tag{47}$$

There exists a scalar $\bar{\gamma}_{i,l} > 0$ that satisfies $|\gamma_{i,l}(\cdot)| < \bar{\gamma}_{i,l}$. Then by substituting (45)~(47) to (44), we get

$$\dot{V}_{i,M} \leq -\sum_{l=1}^{M} c_{i,l} \log \frac{k_{bl}^2}{k_{bM}^2 - \vartheta_{i,M}^2} - \sum_{l=1}^{M} \frac{\sigma_{i,l}\tilde{\theta}_{i,l}^2}{2} - \sum_{l=2}^{M} \left(\frac{1}{\tau_{i,l}} - \frac{\bar{\gamma}_{i,l}^2}{2} - \frac{1}{2} \right) \lambda_{i,l}^2 + \Lambda_i \tag{48}$$

where

$$\Lambda_i = \frac{1}{2} \sum_{l=1}^{M} \left(p_{i,l}^2 + \bar{\varepsilon}_{i,l}^2 \right) + \sum_{l=1}^{M} \frac{\sigma_{i,l}\theta_{i,l}^{*2}}{2} + \frac{M-1}{2} + 0.2785\epsilon_i \tag{49}$$

With Assumption 1 holding true and virtual control signals (23), (32) and (40), adaptive protocols (24), (33), and (41) and event-triggered adaptive controllers (39), (42) and (43) being considered, we can ensure that the MAS described in (5) meets the following conditions: 1) All signals in the system are semi-globally uniform and ultimately bounded; 2) The tracking error converges to the bounded neighborhood of the origin and meets the prescribed performance. In addition, there is a lower bound $t^*, t^* > 0$ for the time interval $\{t_{k+1} - t_k\}$ triggered by the event. That is, the Zeno phenomenon will not occur when the adaptive controller is triggered by the event.

Proof. Define a Lyapunov function as

$$V = \sum_{i=1}^{N} V_{i,M} \tag{50}$$

According to (48), we have

$$\dot{V} \leq \sum_{i=1}^{N} \Bigg[-\sum_{l=1}^{M} c_{i,l} \log \frac{k_{bl}^2}{k_{bl}^2 - \vartheta_{i,l}^2} - \sum_{l=1}^{M} \frac{\sigma_{i,l}\tilde{\theta}_{i,l}^2}{2} - \sum_{l=2}^{M} \left(\frac{1}{\tau_{i,l}} - \frac{\bar{\gamma}_{i,l}^2}{2} - \frac{1}{2} \right) \lambda_{i,l}^2 + \Lambda_i \Bigg] \tag{51}$$

Choose design parameters such that $\frac{1}{\tau_{i,1}} - \frac{\bar{\gamma}_{i,l}}{2} - \frac{1}{2} > 0$. Let

$$\Gamma = \min \left\{ 2c_{i,l}, 2\left[\frac{1}{\tau_{i,l}} - \frac{\bar{\gamma}_{i,l}}{2} - \frac{1}{2} \right], \sigma_{i,l} \right\}$$
$$\Lambda = \sum_{i=1}^{N} \Lambda_i \tag{52}$$

Thus (51) can be rewritten as

$$\dot{V}(t) \leq -\Gamma V(t) + \Lambda \tag{53}$$

such that all the signals are semi-globally uniform and ultimately bounded. According to (53), we have

$$\frac{1}{2}\vartheta_{i,l}^2 \leq V(t) \leq \exp(-\Gamma t)V(0) + \frac{\Lambda}{\Gamma}(1 + \exp(-\Gamma t)) \tag{54}$$

According to Lemma 4, we have

$$\lim_{t\to\infty} \parallel y - \bar{y}_0 \parallel \leq \frac{\sqrt{\frac{2\Lambda}{\Gamma}}}{\underline{\sigma}(\mathcal{L} + \mathcal{B})} \tag{55}$$

By selecting appropriate design parameters, the tracking error can converge in a bounded neighborhood centered on the origin. Further, according to $e_i(t) = \omega_i(t) - u_i(t), \forall t \in [t_k, t_{k+1})$, we have

$$\frac{\mathrm{d}|\varrho(t)|}{\mathrm{d}t} = \frac{\mathrm{d}}{\mathrm{d}t}(\varrho \times \varrho)^{\frac{1}{2}} = \mathrm{sign}(\varrho)\dot{e}_i \leq |\dot{\omega}_i| \tag{56}$$

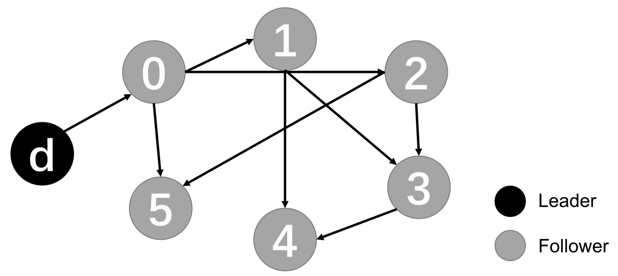

Fig. 2. Directed communication topology with 6 followers and 1 leader.

Because all the signals in the system are bounded, there must be a constant κ, which makes $|\dot{\omega}_i| \leq \kappa$. Based on $e_i(t_k) = 0, \lim_{t\to t_{k+1}} \varrho(t) = m_i$, it can be concluded that the lower bound t^* of the event-triggered time interval satisfies $t^* \geq m_i/\kappa$. It can be proved that the Zeno phenomenon (Ceragioli, 2009) will not occur in the event trigger mechanism proposed in this paper.

4. NUMERIC SIMULATION

This section presents two leader-following simulation experiments on a MAS. As shown in Fig. 2, the network communication topology of the system includes 1 leader and 6 follower agents.

4.1 Simulation 1

Without loss of generality, we assume the weights of the edges communicating with each other are both 1, and the dynamic models of the leader and followers are third-order uncertain nonlinear systems:

$$\begin{aligned} \dot{x}_{i,1}(t) &= x_{i,2}(t) \\ \dot{x}_{i,2}(t) &= x_{i,3}(t) - \sin x_{i,1} - x_{i,2}(t) \\ \dot{x}_{i,3}(t) &= -0.1 * x_{i,2} - 0.2 * x_{i,3} + u_i(t) \\ y_i(t) &= x_{i,1}(t) \end{aligned}$$

Choose the initial states of the leader ($\boldsymbol{x}_0$) and the 5 follower agents ($\boldsymbol{x}_0, \boldsymbol{x}_1, \boldsymbol{x}_2, \boldsymbol{x}_3, \boldsymbol{x}_4, \boldsymbol{x}_5$) as

$$\begin{aligned} \boldsymbol{x}_0 &= [x_{0,1}, x_{0,2}, x_{0,3}]^{\mathrm{T}} = [6, \quad 0.38, \quad 0]^{\mathrm{T}} \\ \boldsymbol{x}_1 &= [x_{1,1}, x_{1,2}, x_{1,3}]^{\mathrm{T}} = [20, \quad -0.76, \quad 0]^{\mathrm{T}} \\ \boldsymbol{x}_2 &= [x_{2,1}, x_{2,2}, x_{2,3}]^{\mathrm{T}} = [0, \quad 0.91, \quad 0]^{\mathrm{T}} \\ \boldsymbol{x}_3 &= [x_{3,1}, x_{3,2}, x_{3,3}]^{\mathrm{T}} = [-5, \quad 0.77, \quad 0]^{\mathrm{T}} \\ \boldsymbol{x}_4 &= [x_{4,1}, x_{4,2}, x_{4,3}]^{\mathrm{T}} = [-2, \quad 0.88, \quad 0]^{\mathrm{T}} \\ \boldsymbol{x}_5 &= [x_{5,1}, x_{5,2}, x_{5,3}]^{\mathrm{T}} = [9, \quad 0.33, \quad 0]^{\mathrm{T}} \end{aligned}$$

Let the desired trajectory of the leader agent be

$$y_d = \sin(t)$$

The initial neural network activation function is initialized with random parameters in advance.

The state trajectories of all the agents of the third-order system are shown in Fig. 3 The position states of the 6 homogeneous followers get gradually close to the position state of leader 0. This means the leader-follower consensus tracking of the MAS is achieved.

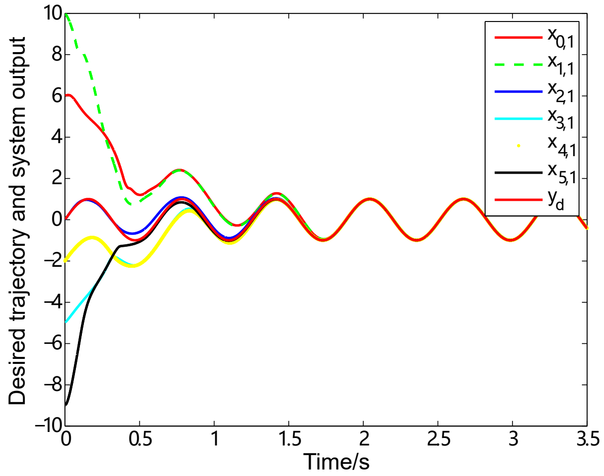

Fig. 3. Tracking trajectory of system state x_1.

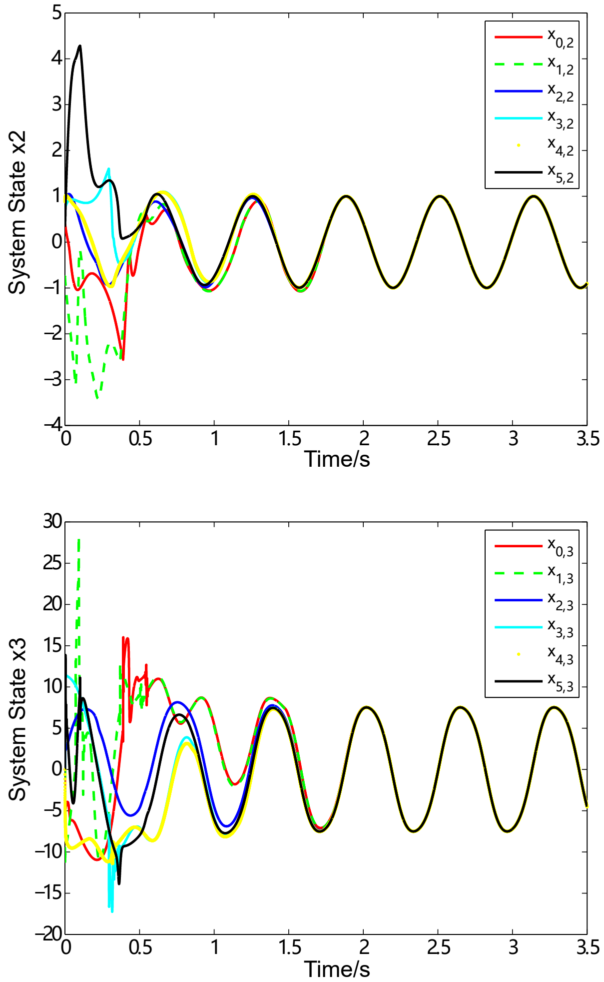

Fig. 4. Tracking trajectory of system state x_2 and x_3.

4.2 Simulation 2

In this simulation, we also the same MAS topology with that in Simulation 1, while the system dynamics are modeled as:

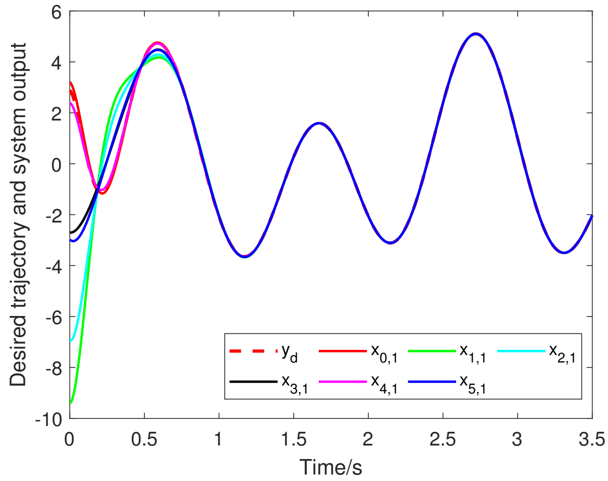

Fig. 5. Tracking trajectory of system state x_1.

$$
\begin{aligned}
\dot{x}_{i,1}(t) &= x_{i,2}(t) \\
\dot{x}_{i,2}(t) &= x_{i,3}(t) + 0.5 \sin x_{i,1} + \cos x_{i,2}(t) \\
\dot{x}_{i,3}(t) &= 0.2 * x_{i,2} + \sin x_{i,3} + u_i(t) \\
y_i(t) &= x_{i,1}(t)
\end{aligned}
$$

Let the initial state of each follower agent be

$$
\begin{aligned}
\boldsymbol{x}_0 &= [x_{0,1}, x_{0,2}, x_{0,3}]^{\mathrm{T}} = [3.4, \quad 0, \quad 8.4]^{\mathrm{T}} \\
\boldsymbol{x}_1 &= [x_{1,1}, x_{1,2}, x_{1,3}]^{\mathrm{T}} = [-9.3, \quad 0, \quad 1.3]^{\mathrm{T}} \\
\boldsymbol{x}_2 &= [x_{2,1}, x_{2,2}, x_{2,3}]^{\mathrm{T}} = [-6.8, \quad 0, \quad -2.4]^{\mathrm{T}} \\
\boldsymbol{x}_3 &= [x_{3,1}, x_{3,2}, x_{3,3}]^{\mathrm{T}} = [-2.7, \quad 0, \quad 1.2]^{\mathrm{T}} \\
\boldsymbol{x}_4 &= [x_{4,1}, x_{4,2}, x_{4,3}]^{\mathrm{T}} = [2.3, \quad 0, \quad -4.5]^{\mathrm{T}} \\
\boldsymbol{x}_5 &= [x_{5,1}, x_{5,2}, x_{5,3}]^{\mathrm{T}} = [-2.5, \quad 0, \quad 4.5]^{\mathrm{T}}
\end{aligned}
$$

Further, define the desired trajectory of the leader agent by

$$y_d = \sin(t) + 2 * \sin(2t + 13)$$

In Fig. 5, we can see that the first order state of all followers can quickly catch up with the leader's state and reach consensus. Fig. 6 also illustrates that the second- and third-order states of the agents can also reach consensus quickly, so the simulation results comprehensively demonstrate the effectiveness of our designed control law.

5. CONCLUSION

This paper investigates the leader-following tracking problem for a class of nonlinear MAS with full-state constraints. In designing the control protocol algorithm, prescribed performance is considered to ensure that the system can obtain the desired steady-state error. Further, radial basis function neural networks are used to process the unknown nonlinear function in a way that ensures the matching condition is satisfied and the unknown nonlinear function is fitted in the controller design. In addition, an event triggering mechanism with a fixed threshold is designed, thereby reducing the computational load on the agents and the cost of communication between them. A dynamical surface technology is also introduced

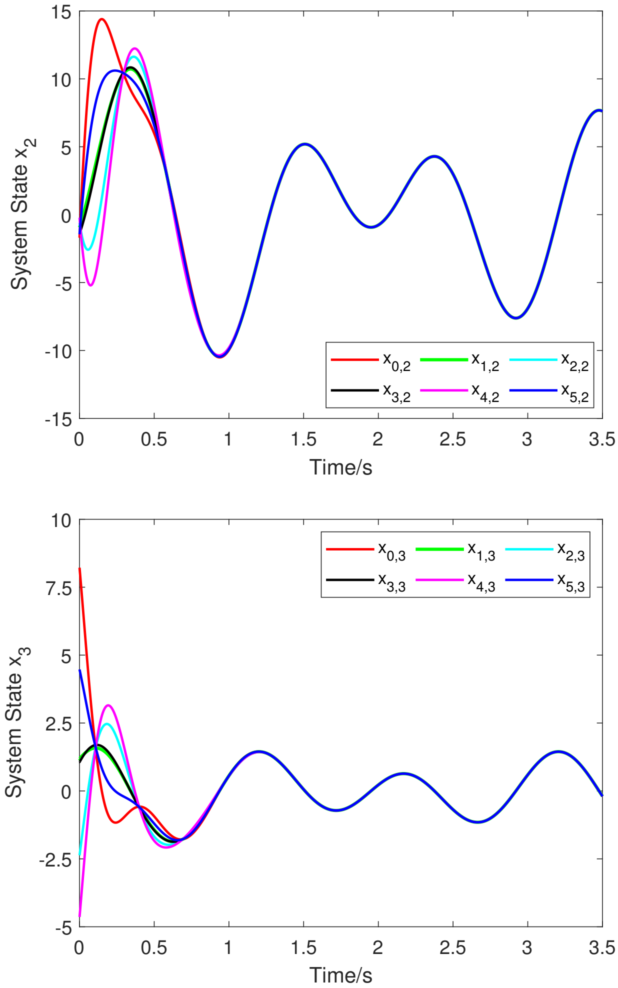

Fig. 6. Tracking trajectory of system state x_2 and x_3.

into the backstepping algorithm to avoid the "computational explosion" problem found in traditional backstepping method. Details are given of how the control algorithm was derived and how its stability is demonstrated. Through two numerical simulations, the control algorithm is shown to be feasible and effective.

REFERENCES

Bechlioulis, C.P. and Rovithakis, G.A. (2008). Robust adaptive control of feedback linearizable mimo nonlinear systems with prescribed performance. *IEEE Transactions on Automatic Control*, 53(9), 2090–2099. doi:10.1109/TAC.2008.929402.

Bechlioulis, C.P. and Rovithakis, G.A. (2014). A low-complexity global approximation-free control scheme with prescribed performance for unknown pure feedback systems. *Automatica*, 50(4), 1217–1226. doi:https://doi.org/10.1016/j.automatica.2014.02.020.

Castro, R., Álvarez, J., and Martínez, J. (2009). Robot formation control using backstepping and sliding mode techniques. In *2009 6th International Conference on Electrical Engineering, Computing Science and Automatic Control (CCE)*, 1–6. IEEE. doi:10.1109/ICEEE.2009.5393430.

Ceragioli, F. (2009). Discrete valued feedback laws and the zeno phenomenon. *Nonlinear Analysis*, 70, 3254–3263. doi:10.1016/j.na.2008.04.028.

Chen, L. and Wang, Q. (2019). Prescribed performance-barrier lyapunov function for the adaptive control of unknown pure-feedback systems with full-state constraints. *Nonlinear Dynamics*, 95, 2443–2459. doi:10.1007/s11071-018-4704-1.

Chen, L., Mei, J., Li, C., and Ma, G. (2020). Distributed leader–follower affine formation maneuver control for high-order multiagent systems. *IEEE Transactions on Automatic Control*, 65(11), 4941–4948. doi:10.1109/TAC.2020.2986684.

Cui, R., Sam Ge, S., Voon Ee How, B., and Sang Choo, Y. (2010). Leader–follower formation control of underactuated autonomous underwater vehicles. *Ocean Engineering*, 37(17), 1491–1502. doi:https://doi.org/10.1016/j.oceaneng.2010.07.006.

Girosi, F. and Poggio, T. (1990). Networks and the best approximation property. *Biological Cybernetics*, 63, 169–176. doi:10.1007/BF00195855.

Isidori, A. (1985). *Nonlinear Control Systems: An Introduction*. Springer.

Krstic, M., Kanellakopoulos, I., and Kokotovic, P.V. (1995). Nonlinear and adaptive control design. *Lecture Notes in Control and Information Sciences*.

Li, Y., Fan, Y., Li, K., Liu, W., and Tong, S. (2021). Adaptive optimized backstepping control-based rl algorithm for stochastic nonlinear systems with state constraints and its application. *IEEE Transactions on Cybernetics*, 1–14. doi:10.1109/TCYB.2021.3069587.

Liu, B., Chu, T., Wang, L., and Xie, G. (2008). Controllability of a leader–follower dynamic network with switching topology. *IEEE Transactions on Automatic Control*, 53(4), 1009–1013. doi:10.1109/TAC.2008.919548.

Ni, W. and Cheng, D. (2010). Leader-following consensus of multi-agent systems under fixed and switching topologies. *Systems and Control Letters*, 59(3), 209–217. doi:https://doi.org/10.1016/j.sysconle.2010.01.006.

Rego, B.S., Adorno, B.V., and Raffo, G.V. (2016). Formation backstepping control based on the cooperative dual task-space framework: A case study on unmanned aerial vehicles. In *2016 XIII Latin American Robotics Symposium and IV Brazilian Robotics Symposium (LARS/SBR)*, 163–168. IEEE. doi:10.1109/LARS-SBR.2016.34.

Song, Y., Zhao, K., and Krstic, M. (2017). Adaptive control with exponential regulation in the absence of persistent excitation. *IEEE Transactions on Automatic Control*, 62(5), 2589–2596. doi:10.1109/TAC.2016.2599645.

Tanner, H., Pappas, G., and Kumar, V. (2004). Leader-to-formation stability. *IEEE Transactions on Robotics and Automation*, 20(3), 443–455. doi:10.1109/TRA.2004.825275.

Wu, Y., Gou, J., Hu, X., and Huang, Y. (2020). A new consensus theory-based method for formation control and obstacle avoidance of uavs. *Aerospace Science and Technology*, 107, 106332. doi:https://doi.org/10.1016/j.ast.2020.106332.

Yu, W., Chen, G., and Cao, M. (2010). Distributed leader–follower flocking control for multi-agent dynamical systems with time-varying velocities. *Systems and Control Letters*, 59(9), 543–552. doi:https://doi.org/10.

1016/j.sysconle.2010.06.014.

Zegers, F.M., Deptula, P., Shea, J.M., and Dixon, W.E. (2022). Event/self-triggered approximate leader-follower consensus with resilience to byzantine adversaries. *IEEE Transactions on Automatic Control*, 67(3), 1356–1370. doi:10.1109/TAC.2021.3074849.

Zhao, K., Song, Y., Ma, T., and He, L. (2018). Prescribed performance control of uncertain euler–lagrange systems subject to full-state constraints. *IEEE Transactions on Neural Networks and Learning Systems*, 29(8), 3478–3489. doi:10.1109/TNNLS.2017.2727223.

Zhou, J., Hu, Q., and Friswell, M.I. (2013). Decentralized finite time attitude synchronization control of satellite formation flying. *Journal of Guidance Control and Dynamics*, 36, 185–195.